Cell Reports
Article

An Anti-inflammatory NOD-like Receptor Is Required for Microglia Development

Celia E. Shiau,[1] Kelly R. Monk,[1,2] William Joo,[1,3] and William S. Talbot[1,*]
[1]Department of Developmental Biology, Stanford University, Stanford, CA 94305, USA
[2]Present address: Department of Developmental Biology, Washington University School of Medicine, St. Louis, MO 63110, USA
[3]Present address: Neuroscience Program, Department of Biology, Stanford University, Stanford, CA 94305, USA
*Correspondence: william.talbot@stanford.edu
http://dx.doi.org/10.1016/j.celrep.2013.11.004

SUMMARY

Microglia are phagocytic cells that form the basis of the brain's immune system. They derive from primitive macrophages that migrate into the brain during embryogenesis, but the genetic control of microglial development remains elusive. Starting with a genetic screen in zebrafish, we show that the noncanonical NOD-like receptor (NLR) *nlrc3-like* is essential for microglial formation. Although most NLRs trigger inflammatory signaling, *nlrc3-like* acts cell autonomously in microglia precursor cells to suppress unwarranted inflammation in the absence of overt immune challenge. In *nlrc3-like* mutants, primitive macrophages initiate a systemic inflammatory response with increased proinflammatory cytokines and actively aggregate instead of migrating into the brain to form microglia. NLRC3-like requires both its pyrin and NACHT domains, and it can bind the inflammasome component apoptosis-associated speck-like protein. Our studies suggest that NLRC3-like may regulate the inflammasome and other inflammatory pathways. Together, these results demonstrate that NLRC3-like prevents inappropriate macrophage activation, thereby allowing normal microglial development.

INTRODUCTION

As the only immune cells dedicated to the defense of the CNS, microglia have unique functions and developmental origins (Aguzzi et al., 2013; Ransohoff and Cardona, 2010). Microglia are extremely sensitive to signs of infection, injury, and disease of the brain, and they can respond rapidly, depending on the nature of the stimulus (Ransohoff and Perry, 2009; Perry et al., 2010). After infection, for example, microglia engulf pathogens and initiate an immune response, and they can clear cell corpses and promote healing after injury to the CNS. Microglia also interact with and eliminate neuronal synapses, and they may therefore modulate neuronal connectivity (Paolicelli et al., 2011; Peri and Nüsslein-Volhard, 2008; Schafer et al., 2012; Ransohoff and Cardona, 2010). Unlike other CNS cell types, which derive from the neuroectoderm, microglia arise from a subset of primitive macrophages that migrates from the yolk sac into the brain during embryogenesis (Ginhoux et al., 2010, Herbomel et al., 2001). Primitive macrophages from the yolk sac in mouse (Ginhoux et al., 2010) and zebrafish (Herbomel et al., 1999, 2001) enter the brain prior to definitive hematopoiesis and differentiate into microglia that remain in the brain thereafter (Ginhoux et al., 2010). Because microglia in the adult brain derive from the early embryonic macrophage population, early disruption of microglia in the embryo may impair the immune system of the developing and mature CNS. The cellular and molecular mechanisms, however, that mediate the specification, migration, and differentiation of developing microglia remain elusive.

NOD-like receptors (NLRs) are intracellular pattern-recognition receptors that regulate innate immunity and inflammatory processes (Chen et al., 2009; Davis et al., 2011; Mason et al., 2012). They can respond to pathogens and cellular stress by triggering caspase-1-dependent inflammatory signaling or by activating NF-κB to promote production of proinflammatory cytokines (Chen et al., 2009; Davis et al., 2011). Upon recognizing various ligands, putatively through their C-terminal leucine-rich repeats (LRRs) (Chen et al., 2009; Davis et al., 2011; Mason et al., 2012), NLRs form large multiprotein complexes by self-oligomerization at their central NACHT domain. Activated NLRs recruit other proteins through homotypic interactions with their N-terminal domains, typically either a pyrin or a CARD domain, to activate NF-κB through the NODosome pathway or caspase-1 through the inflammasome mechanism (Chen et al., 2009; Davis et al., 2011). Mutations causing aberrant NLR signaling are linked to numerous human inflammatory disorders, such as inflammatory bowel disease, vitiligo, sarcoidosis, and cryopyrin-associated periodic syndromes (Chen et al., 2009; Davis et al., 2011; Mason et al., 2012), underscoring the importance of curbing inflammatory signaling mediated by the NLRs. Recent studies have shown that NLRC3 and NLRP12 can suppress inflammation after challenge by lipopolysaccharide (LPS) or infection (Schneider et al., 2012; Allen et al., 2012; Zaki et al., 2011). Despite the far-reaching roles of the NLRs in controlling innate immunity, the mechanisms that regulate their

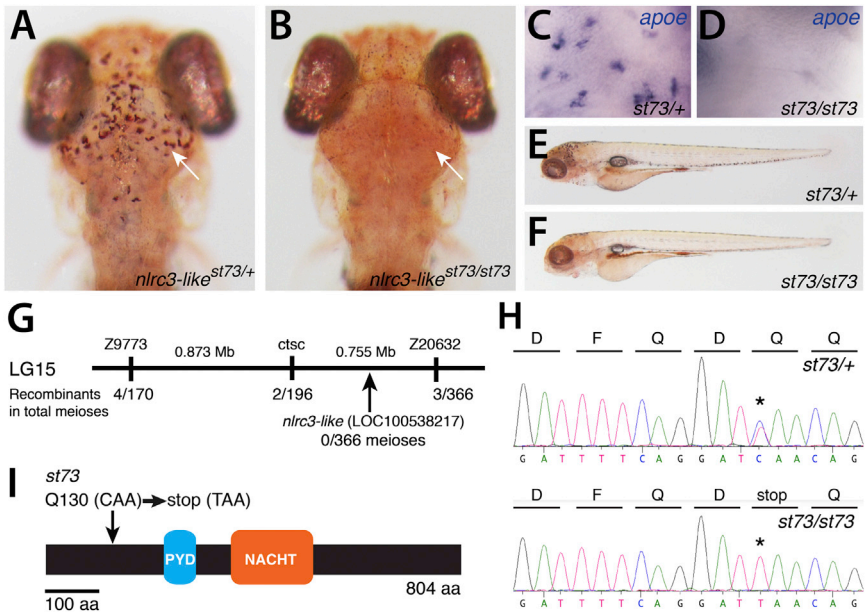

Figure 1. Lack of Microglia in *nlrc3-like* Mutants

(A and B) Live 5 dpf zebrafish larvae were stained by neutral red to visualize microglia in the brain.

(A) Heterozygous *st73*/+ larva (arrow points to microglia around optic tectum) is shown.

(B) Homozygous *st73* larvae have no microglia (arrow). Dorsal views; anterior is to the top.

(C and D) Microglial marker *apoe* expression at 5 dpf in the brain is shown.

(E and F) Neutral red-stained heterozygous (E) and homozygous mutant (F) shows normal whole-animal morphologies at 5 dpf. Lateral views; anterior is to the left.

(G) Genetic and physical map of the *st73* locus.

(H) Sequence chromatogram shows the lesion (asterisks) in the coding sequence of *nlrc3-like* (LOC100538217).

(I) The *st73* mutation introduces a premature stop codon near the 5′ end of the open reading frame of *nlrc3-like*.

See also Figure S1.

functions and maintain homeostasis in the absence of infection are not well understood.

Starting with a genetic screen for mutations that disrupt microglia in zebrafish, we identified a noncanonical NLR, *nlrc3-like*, that is essential for microglia formation in zebrafish. Our analysis demonstrates that *nlrc3-like* prevents runaway inflammation during embryogenesis and thereby allows the development of microglia. In *nlrc3-like* mutants, primitive macrophages adopt an inflammatory phenotype instead of migrating into the brain to differentiate as microglia. In addition, *nlrc3-like* mutants have systemic inflammation, as evidenced by elevation of proinflammatory cytokines and recruitment of neutrophils into the brain and circulation. Transgenic expression of the wild-type *nlrc3-like* gene in macrophages rescued microglia in the mutants, indicating that the gene acts autonomously in macrophages. Our results demonstrate that *nlrc3-like* serves as an essential, cell-autonomous checkpoint in primitive macrophages that prevents unwarranted inflammation in the absence of overt immune challenges and allows the normal development of microglia.

RESULTS

nlrc3-like Is Essential for Microglia Development

In a genetic screen in zebrafish, we identified *st73* as a recessive mutation that eliminated microglia (Figures 1A and 1B). At 5 days postfertilization (dpf), homozygous *st73* mutant larvae lacked microglial cells (Figures 1A–1D) but did not have any apparent anatomical defects (Figures 1E and 1F). High-resolution meiotic mapping localized the *st73* mutation to a 1.63 Mb region of linkage group 15 (LG15) (Figure 1G). Among the genes in this interval is *nlrc3-like* (LOC100538217) (Figure 1G), which encodes an atypical member of the NLR family that contains the canonical pyrin (PYD) and NACHT domains but lacks the common LRRs thought to be important for ligand sensing and self-inhibition (Davis et al., 2011; Mason et al., 2012). NLRC3-like belongs to an expanded subfamily of teleost NLRs that shares significant similarity to the human NLRC3 (or Nod3), based on sequence comparisons of the NACHT domain (Laing et al., 2008; Hughes, 2006). Sequence analysis identified a nonsense mutation in *nlrc3-like* near the 5′ end of the open reading frame (Figures 1H and 1I). All *st73* mutants analyzed were homozygous for this lesion (n = 300). Injection of synthetic mRNA encoding the wild-type NLRC3-like protein can fully rescue microglia in *st73* mutants and had no effect on wild-type siblings (Figure S1). On the basis of mapping, the identification of the nonsense lesion, and RNA rescue experiments, we conclude that *st73* is a loss-of-function mutation in the *nlrc3-like* gene.

Abnormal Migration and Inflammatory Activation of Macrophages in *nlrc3-like* Mutants

To define the role of *nlrc3-like* in microglia development, we examined different stages of microglia development starting from the formation of primitive macrophages to differentiation of microglia (20–60 hr postfertilization [hpf]) using markers specific to macrophages (*microfibrillar-associated protein 4* [*mfap4*] and *macrophage-expressed gene 1* [*mpeg1*]) (Ellett et al., 2011; Zakrzewska et al., 2010) and all leukocytes (*l-plastin*) (Meijer and Spaink, 2011). We detected no difference in macrophage, neutrophil, or overall leukocyte number and distribution, vasculature formation, or blood circulation between mutants and their wild-type siblings at early time points up to 24 hpf (Figure S2; data not shown). By 2 dpf, however, mutant macrophages aggregated in large clusters on the yolk (Figures 2A–2C and S2). Time-lapse imaging revealed that macrophages actively migrated toward and joined these aggregates in the mutant, in clear contrast to wild-type siblings, in which no aggregation occurred (Figure 2C; Movies S1 and S2). Other macrophages in mutants migrated from the yolk, but they often still formed small clusters (Figure 2E, arrowheads). These macrophages

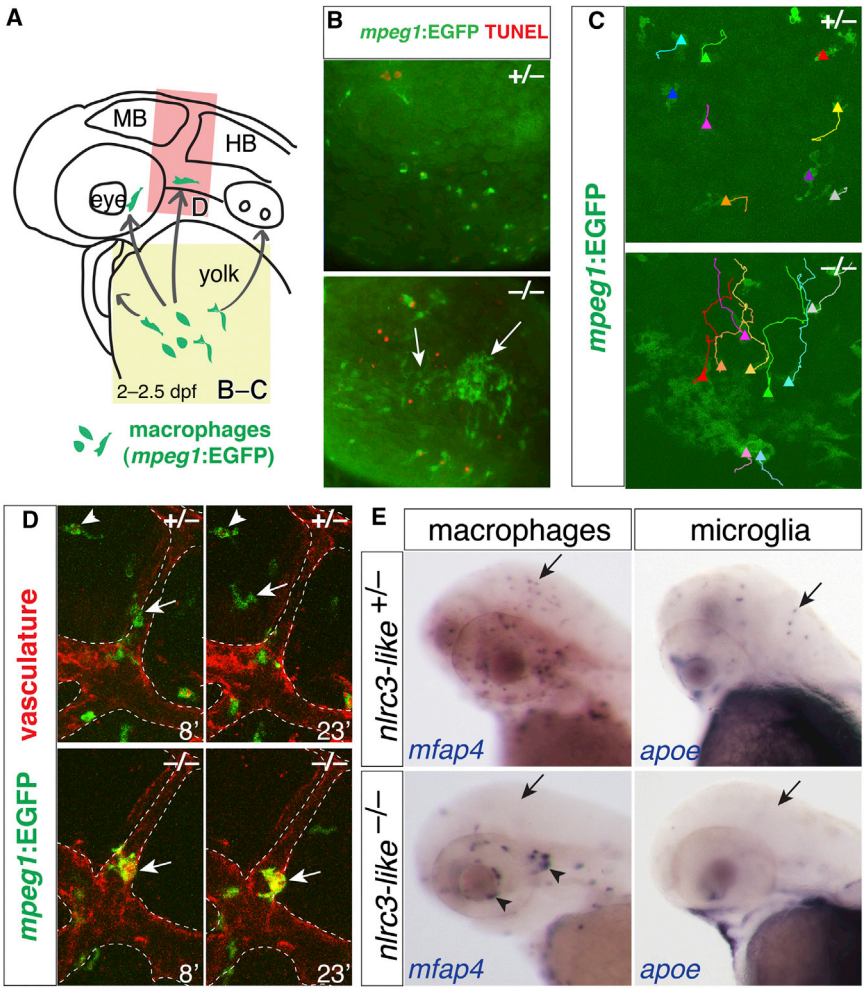

Figure 2. Aberrant Migration of Primitive Macrophages in *nlrc3-like*$^{-/-}$ Mutants

(A) Diagram shows the stereotypical migration route of macrophages from yolk sac to embryo proper (arrows).

(B) Fluorescent images show abnormal active coalescence of yolk sac macrophages (*mpeg1:EGFP*+ in green, arrows) that overlap with apoptotic marker TUNEL in red in mutants (bottom panel; n = 12/12), which does not occur in wild-type (top panel; n = 11/11). Region of imaging is indicated by yellow box in (A).

(C) Trajectories of individual yolk sac macrophages are shown using the MTrackJ cell-tracking tool, where the end point is indicated by a solid-triangle marker. See Movies S1 and S2 for the time-lapse series.

(D) Time-lapse imaging shows the head region (red box in A) where macrophages are expected to migrate into the brain, using transient transgenesis of the *mpeg1:EGFP* construct labeling macrophages in green and the stable transgene *kdrl:mCherry-CAAX* to visualize the vasculature in red. Imaging shows macrophages entering the brain in wild-type siblings (top) but not mutant (bottom). The numbers indicate the time in minutes. In the top panels, the arrowhead points to a macrophage that has taken up residence in the brain to become a microglial cell; the arrow points to another macrophage migrating into the brain. In the bottom panels, the arrow points to a mutant macrophage that does not enter the brain and remains associated with vasculature (as demarcated by dotted lines). See Movies S3 and S4.

(E) Whole-mount in situ hybridization at 2.5 dpf shows macrophage *mfap4*+ and microglial *apoe*+ cells in wild-type heterozygous embryos (arrows), but not in mutants (arrows). Aberrant macrophage clusters form near cranial vasculature in mutants (arrowheads). MB, midbrain; HB, hindbrain.

See also Figure S2 and Movies S1–S4.

typically did not enter the brain parenchyma in the mutants but, instead, remained associated with the vasculature (Figure 2D; Movies S3 and S4). Macrophage and microglia markers (*mfap4* and *apoe*, respectively) confirmed the absence of brain macrophages and microglia through 2.5 dpf, even though peripheral macrophages were present (Figure 2E). The formation of aggregates is characteristic of macrophages activated by infection or injury (Renshaw and Trede, 2012). We also observed that macrophages in mutants formed large cytoplasmic vacuoles, often several per cell (Figures 3A–3C), and that a higher fraction of macrophages were TUNEL positive at 2.5 dpf in mutants than in sibling controls (Figures 3C–3E). TUNEL-positive macrophages in the mutants exhibited condensed apoptotic nuclei (Figure 3D) or cellular breakdown (Figure 3E), two characteristics of an inflammatory form of apoptosis called pyroptosis (Lamkanfi and Dixit, 2010; Lage et al., 2013). The number of macrophages in the mutants declined significantly by 3–4 dpf (Figure 3F), consistent with an increase in apoptotic macrophages. The active aggregation, vacuolation, and pyroptotic death of macrophages in *nlrc3-like* mutants resemble phenotypes previously described for macrophages responding to infection (Mujawar et al., 2006; Siracusa et al., 2008; Lage et al., 2013; Renshaw and Trede, 2012), suggesting that *nlrc3-like* mutant macrophages are activated despite the absence of overt infection.

Because macrophage activation is a prominent component of the inflammatory immune response after infection or injury (Mosser and Edwards, 2008), we examined whether the macrophage abnormalities in *nlrc3-like* mutants were linked to inappropriate inflammation. Using quantitative PCR (qPCR), we found a highly significant increase in all proinflammatory cytokines tested (*il-1β*, *il-8*, *il-12a*, and *tnfα*) (Rock et al., 2010), but no detectable change in expression of the *β-actin* control or the anti-inflammatory cytokine *il-10* (Moore et al., 2001) in the mutants relative to wild-type siblings (Figure 3G; data not shown). The highly elevated expression of proinflammatory cytokines indicated that macrophages in the mutants were activated in the context of an inflammatory environment. These inappropriately activated embryonic macrophages (microglia precursor cells) do not migrate properly and undergo premature cell death, thus accounting for the lack of microglia in *nlrc3-like* mutants.

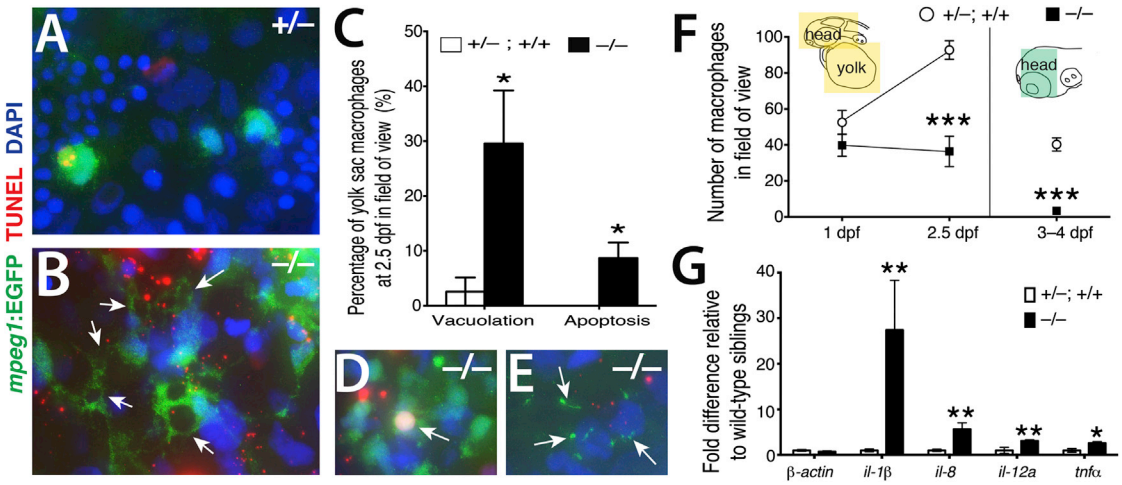

Figure 3. Inappropriate Inflammatory Activation of Macrophages in *nlrc3-like*$^{-/-}$ Mutants

(A and B) High-magnification images show striking cell morphology differences between yolk sac macrophages of wild-type (A) and mutant (B). Macrophages in the mutants have multiple, large vacuoles (arrows).

(C) Plot shows significantly higher percentages of primitive macrophages (*mpeg1-EGFP*+) exhibiting vacuolation (one or more large cytoplasmic vacuoles; p = 0.047) and cell death (overlap of TUNEL staining with macrophage DAPI staining; p = 0.037) in *nlrc3-like*$^{-/-}$ mutants (n = 5 embryos) compared with siblings (n = 6 embryos). Statistical significance was determined by the two-tailed Student's t test.

(D and E) Examples of dying mutant macrophages exhibiting apoptosis (arrow in D), and cellular breakdown (arrows in E) are shown.

(F) Plot shows macrophage number over time. Diagram indicates the region of quantification (colored boxes): n = 5 for each genotype at 1 and 2.5 dpf, p = 0.0009 at 2.5 dpf; at 3–4 dpf, n = 7 siblings and n = 3 mutants ($p = 2 \times 10^{-5}$).

(G) Graph shows relative mRNA levels of proinflammatory cytokines by qPCR comparing mutants (n = 6) to wild-type siblings (n = 6) at 3 dpf. p = 0.70 (*β-actin*), p = 0.002 (*il-1β*), p = 0.004 (*il-8*), p = 0.008 (*il-12a*), and p = 0.03 (*tnfα*).

n, number of independent embryos analyzed. Error bars show SEM. *p < 0.05, **p < 0.01, and ***p < 0.001. All p values are two tailed.

Systemic Inflammation in *nlrc3-like* Mutants

The abnormal activation of macrophages in *nlrc3-like* mutants raised the possibility of a broader dysregulation of the immune system. To investigate whether other immune cells are disrupted in *nlrc3-like* mutants, we examined neutrophils, the only other mature leukocyte present during embryonic stages, before the adaptive immune system is functional (Lam et al., 2004). Whereas neutrophils were excluded from the brain of wild-type embryos, they aberrantly infiltrated the brains of *nlrc3-like* mutants (Figure 4), as demonstrated by examination of the neutrophil markers myeloperoxidase (mpo) and lysozyme C (lyz) (Meijer and Spaink, 2011). In vivo time-lapse imaging of the neutrophil reporter transgene *lyz:EGFP* (Hall et al., 2007) (Figures 4A–4F; Movies S5 and S6) revealed neutrophils freely roaming in the brain of *nlrc3-like* mutants. Quantitation of lyz:EGFP+ neutrophil numbers revealed a significant number of brain neutrophils in *nlrc3-like* mutants, compared with essentially none in wild-type siblings (Figure 4G). Transverse sections confirmed the mislocalization of mutant neutrophils in the brain parenchyma and around vasculature (Figure S3). In addition to brain infiltration, live imaging in *nlrc3-like* mutants also revealed a highly significant increase of neutrophils in circulation (Figures 4H–4J; Movies S7 and S8), starting as early as 1.5 dpf, when primitive macrophages begin to enter the brain in wild-type embryos. Using markers to distinguish neutrophils (*lyz:EGFP*+ and pan-leukocyte marker L-plastin+) and macrophages (L-plastin+ only), we also found that neutrophils joined the aberrant aggregates of macrophages described above (Figures 2B, 2C, and 4K). The increase of neutrophils in circulation, infiltration of neutrophils into the brain, intermixing of neutrophils and macrophages in abnormal aggregates, and extremely high levels of proinflammatory cytokines collectively indicate systemic inflammation in *nlrc3-like* mutants.

nlrc3-like Acts Autonomously in Macrophages to Mediate Normal Microglia Development

In light of such systemic inflammation, we sought to determine whether NLRC3-like acts within macrophages or in other cell types. Using transient Tol2-mediated transgenesis in *nlrc3-like* mutants, we introduced constructs that expressed either the wild-type *nlrc3-like* or control *mCherry* coding sequence in skin, neurons, neutrophils, or macrophages using cell-type-specific regulatory elements (Figures 5A, 5B, and S4). Expression of the wild-type *nlrc3-like* gene in macrophages rescued microglia (>20 microglia/embryo; 24% of the mutants, n = 55), but expression in the other cell types did not (Figure 5). Partial rescue (10–20 microglia/embryo) was also observed in 11% of mutants injected with the macrophage expression construct (Figure 5B). There was one case of partial rescue with the neuronal *nlrc3-like* expression construct (among 25 mutants examined), perhaps due to leaky promoter expression (Figure 5B). No rescue or partial rescue was obtained with any of the control mCherry expression constructs (Figure 5B). Driving *nlrc3-like* expression using the myeloid lineage-specific *pu.1/spi1-GAL4* line also rescued microglia in the mutants, providing further evidence that *nlrc3-like* is required in macrophages (Figure S4).

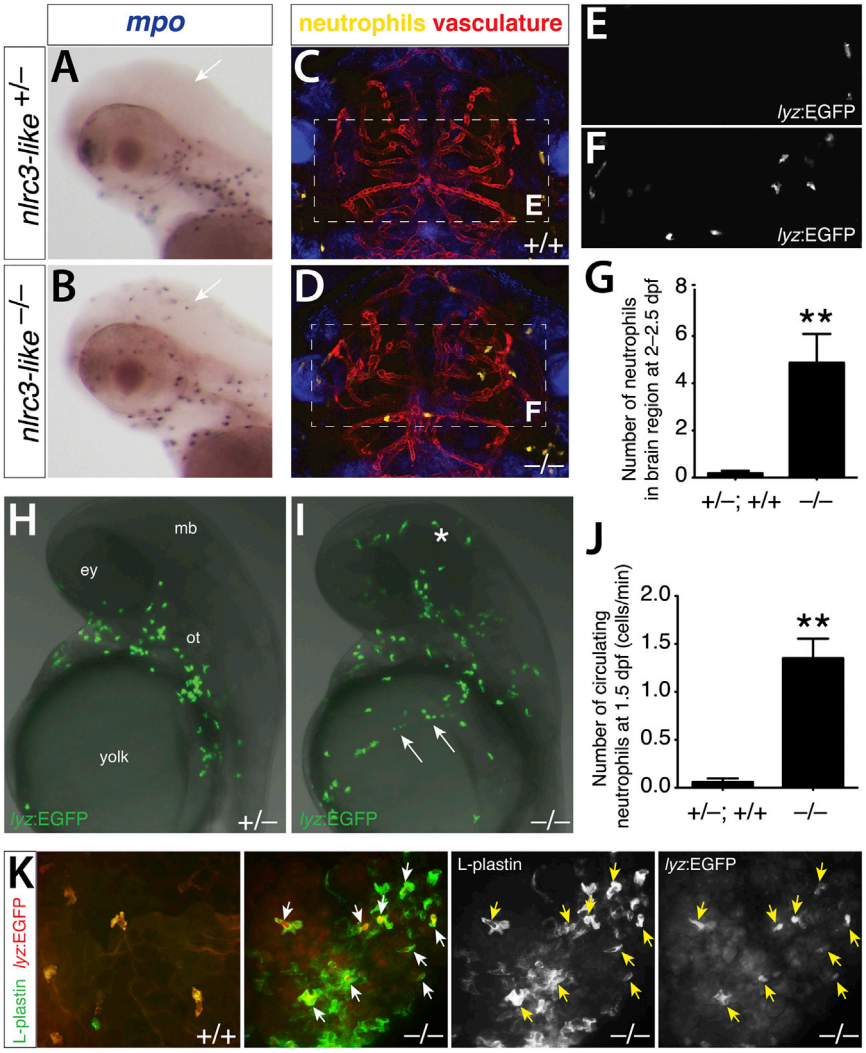

Figure 4. Systemic Inflammation in *nlrc3-like*$^{-/-}$ Mutants in the Absence of Infection or Injury

(A and B) Neutrophil-specific marker *mpo* shows no brain neutrophils in wild-type siblings (arrow, A) but abundant infiltration in mutants (arrow, B). Lateral views, anterior to the left.

(C and D) Representative frames from time-lapse imaging in the intact 2.5 dpf embryos (see Movies S5 and S6) show wandering neutrophils (*lyz:EGFP*) in the brain of mutants (D) but none in wild-type (C), with reference to vasculature (*kdrl:mCherry-CAAX*). Dorsal views, anterior to the top.

(E and F) Higher magnification shows GFP channel alone (dotted-box region in C and D, respectively).

(G) Plot shows that high numbers of neutrophils infiltrate the brain in mutants (n = 15) but nearly zero in wild-type (n = 16; p = 0.0018).

(H and I) Representative images show live imaging of neutrophils at 1.5 dpf in wild-type sibling (H) and in mutant (I). (I) Mutant embryos show large numbers of neutrophils in brain (asterisk) and circulation (arrows). Lateral views, anterior to the top. ey, eye; mb, midbrain; ot, otic vesicle.

(J) Plot shows significantly higher numbers of circulating neutrophils in mutants (n = 4) compared with wild-type (n = 5; p = 0.0083).

(K) Neutrophils (*lyz:EGFP* as pseudocolored in red) are closely intermixed with the aberrantly coalescing macrophages (L-plastin expression only as shown in green) in the mutants, whereas wild-type neutrophils are dispersed and not clustered with macrophages.

n, number of embryos analyzed. Error bars show SEM. **p < 0.01. All p values are two tailed.

See also Figure S3 and Movies S5–S8.

nlrc3-like Continues to Be Required after Microglial Progenitors Enter the Brain and Differentiate

To test whether *nlrc3-like* is required after macrophages have entered the brain and differentiated as microglia, we transiently restored wild-type *nlrc3-like* expression by synthetic mRNA injection at the one-cell stage. Injection of *nlrc3-like* mRNA into mutants can restore microglia at 5 dpf and earlier stages (Figure S1; data not shown). By contrast, at 6 dpf, no mutants injected with *nlrc3-like* mRNA exhibited wild-type numbers of microglia (n = 45), and more than half of the injected mutants had no microglia detectable by neutral red staining (Figure 5C). Consistent with a continuous requirement in microglia development, *nlrc3-like* mRNA is expressed at every stage we examined in wild-type embryos, from embryogenesis through the early larval period (1–9 dpf; Figure S5). These data indicate that *nlrc3-like* continues to be required to maintain the proper number of microglia at later stages.

To assess inflammation in *nlrc3-like* mutants at later stages, we measured cytokine expression by qPCR. As at 3 dpf (Figure 3G), transcripts for *il-1β*, *il-8*, and *tnfα* were significantly elevated in *nlrc3-like* mutants at 6 dpf, but *il-12a* expression was similar to wild-type siblings (Figure 5D). To determine whether early expression of wild-type *nlrc3-like* is sufficient to suppress inflammation at later stages, we also examined cytokine levels in mutants injected with *nlrc3-like* mRNA. Proinflammatory cytokine expression at 6 dpf was elevated relative to wild-type controls, and the extent of the increase correlated with the number of microglia in the transiently rescued mutants (Figure 5D). In these transient rescue experiments, mutants with more than ten detectable microglia had significantly lower levels of *il-8* and *tnfα* (p = 0.01 and 0.03, respectively) than mutants with no microglia. These data indicate that *nlrc3-like* continues to be required to suppress inflammation and allow the development of the full population of microglia, even after microglia progenitors have entered the brain and differentiated.

Macrophages Are Required for Increased Inflammatory Signaling in *nlrc3-like* Mutants

The autonomous action of *nlrc3-like* in the macrophage lineage and the integral roles of macrophages in mediating and responding to inflammation (Rock et al., 2010; Mosser and

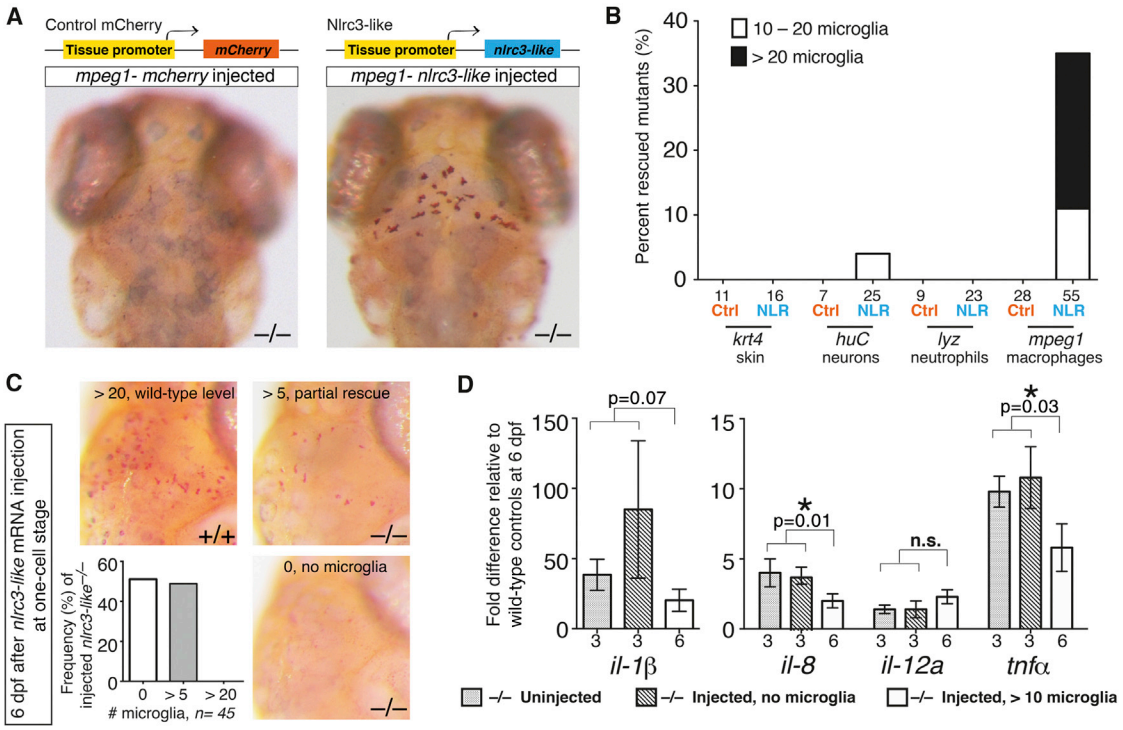

Figure 5. *nlrc3-like* Has an Autonomous and Continuous Function in Macrophages that Become Microglia

(A) Top view is a diagram of transgenic constructs driving either control *mCherry* or *nlrc3-like* expression by tissue-specific gene promoters in skin (*keratin 4/krt4*), neurons (*elavl3/huC*), neutrophils (*lyz*), *or* macrophages (*mpeg1*). Bottom view is representative images showing rescue of neutral red-positive microglia in *nlrc3-like*$^{-/-}$ mutants when expression of wild-type *nlrc3-like* is restored in macrophages (right), but not by control *mCherry* expression (left).

(B) Plot quantifies the percentage of microglia rescue using different tissue-specific expression vectors. Ctrl, control mCherry injected; NLR, *nlrc3-like* construct injected.

(C) Images and plot show microglia by neutral red staining at 6 dpf, after *nlrc3-like* mRNA injection at the one-cell stage. Injected *nlrc3-like*$^{-/-}$ mutants show no microglia or partial rescue (more than five microglia) at 6 dpf, but no mutants are rescued to the wild-type level. In contrast, RNA injection does fully rescue microglia in some mutants at earlier stages (Figure S1).

(D) Graph shows relative proinflammatory transcript levels after transient rescue of *nlrc3-like*$^{-/-}$ mutants by injection of wild-type *nlrc3-like* mRNA at one-cell stage. Injected mutants with no microglia at 6 dpf have elevated levels of proinflammatory cytokine transcripts that are similar to uninjected mutants. In contrast, mutants with partial rescue of microglia at 6 dpf have lower levels of *il-8* and *tnf-α* expression, indicating that the number of microglia correlates inversely to the extent of inflammatory cytokine expression. Individual plots are normalized to their corresponding wild-type siblings, either uninjected or injected.

Numbers below bar graphs represent n, number of embryos analyzed. Error bars show SEM. *p < 0.05, one-tailed Student's t test. n.s., not significant.

See also Figures S4 and S5.

Edwards, 2008) prompted us to ask whether macrophages contributed to the systemic inflammation in *nlrc3-like* mutants. We thus examined proinflammatory cytokine expression after ablating macrophages in *nlrc3-like* mutants with a morpholino (MO) against *interferon regulatory factor-8* (*irf8*) (Li et al., 2011) (Figure 6A). Macrophage ablation reduced *il-1β* expression in *nlrc3-like* mutants to wild-type levels (Figure 6B). In control assays, macrophage ablation in wild-type embryos did not alter *il-1β* levels, whereas *il-1β* expression remained elevated in unablated mutants (Figure 6B), consistent with our previous analysis (Figure 3G). All other proinflammatory cytokines (*il-8*, *il12a*, and *tnfα*) examined were also comparable to wild-type levels in macrophage-ablated mutants (Figure 6B). Taken together, these results demonstrate that macrophages are required for the increased inflammatory signaling in *nlrc3-like* mutants.

NLRC3-like Requires Both the Pyrin and NACHT Domains and May Interact with the Inflammasome Component ASC

The inflammatory phenotypes of *nlrc3-like* mutants suggested that this unusual NLR family member might regulate the production of proinflammatory cytokines and induction of pyroptosis by inhibiting the inflammasome (Davis et al., 2011). Previous in vitro studies indicate that cellular and viral proteins with similar domain organizations, containing only the PYD or PYD combined with NACHT, can inhibit the inflammasome through homotypic interactions with other inflammasome components containing these domains (Dorfleutner et al., 2007a, b; Imamura et al., 2010; Stehlik et al., 2003). To examine the possibility that NLRC3-like interacts with components of the inflammasome, we asked whether NLRC3-like protein can bind to the PYD-containing adaptor protein of the

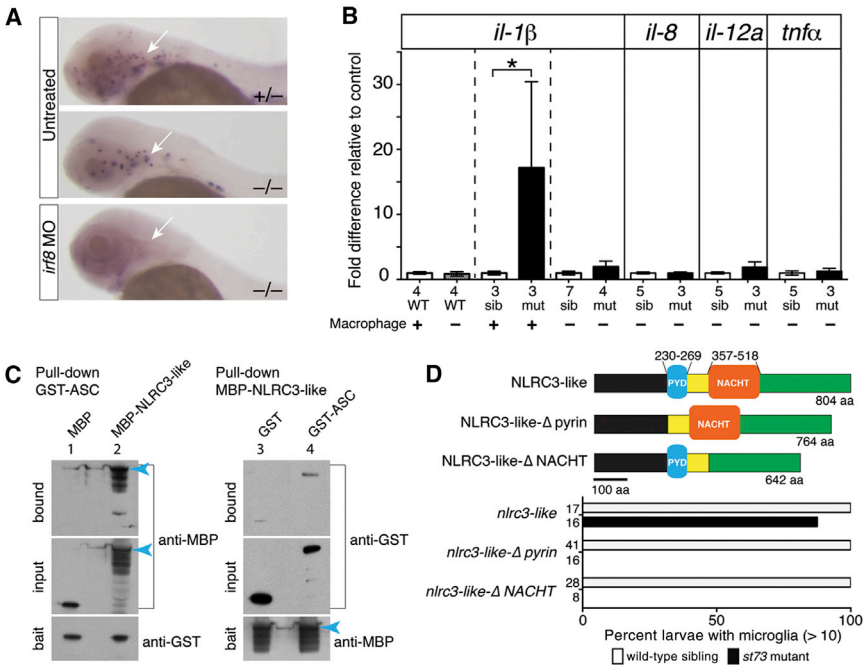

Figure 6. NLRC3-like Negatively Regulates Inflammatory Signaling through Macrophages and May Interact with the Inflammasome Component ASC and Other Pyrin and NACHT-Containing Proteins

(A) Macrophage *mfap4* expression shows complete macrophage ablation by *irf8* MO injection at 2 dpf (arrow). Injected wild-type embryos show complete loss of neutral red-positive microglia (n = 29/29; data not shown).

(B) Graph shows relative *il-1β* mRNA levels, with pairwise comparisons indicated by the dotted lines. Depletion of macrophages in *nlrc3-like* mutants (mut) reduces *il-1β* and other proinflammatory cytokine levels similar to wild-type (WT) levels. sib, siblings.

(C) SDS-PAGE analyses of reciprocal pull-down assays show binding of zebrafish ASC with NLRC3-like (lanes 2 and 4) and minimal binding to tag-alone controls (lanes 1 and 3). MBP-tagged full-length NLRC3-like runs near 160 kDa (blue arrowhead) with several smaller processed forms; GST-ASC at 50 kDa; MBP alone from pMAL-c2X vector at 50 kDa; and GST alone at 30 kDa. Blot shows 0.4% of the input prey protein per lane.

(D) Top view is a schematic of the wild-type NLRC3-like protein and deletion versions: NLRC3-like- Δpyrin with deletion at amino acids (aa) 230–269 and NLRC3-like-ΔNACHT with deletion at aa 357–518. At the bottom is a bar graph showing rescue of *st73* mutants (87.5%, n = 16) by injection of mRNA encoding wild-type NLRC3-like, but none using the mutant constructs. Numbers at left edge of bar graphs represent n, number of embryos analyzed. Error bars show SEM. *p < 0.05.

inflammasome, apoptosis-associated speck-like protein (ASC) (Davis et al., 2011). Reciprocal pull-down assays showed that glutathione S-transferase (GST)-tagged zebrafish ASC and maltose-binding protein (MBP)-tagged NLRC3-like can bind (Figure 6C). The unusual pyrin-NACHT structure of NLRC3-like, the systemic inflammation in *nlrc3-like* mutants, and the potential interaction between the NLRC3-like and ASC proteins suggest that NLRC3-like may negatively regulate inflammasome activity or other pathways mediating inflammatory signaling that involve ASC (Sarkar et al., 2006; Kolly et al., 2009).

To determine which domains may be essential for *nlrc3-like* function, we performed a structure-function analysis. We designed deletion constructs that express mRNAs encoding NLRC3-like proteins that lack either the NACHT domain (*Nlrc3-like-ΔNACHT*) or the pyrin domain (*Nlrc3-like-Δpyrin*), which are the two recognizable conserved domains in NLRC3-like. Wild-type *nlrc3-like* mRNA injection can fully rescue microglia in *nlrc3-like* mutants at 3–5 dpf (Figures 6D and S1), and we assayed the ability of mRNAs encoding the deletion mutants to rescue *nlrc3-like* mutants (Figure 6D). Both domains are required to rescue *nlrc3-like* mutants (Figure 6D), providing evidence that the pyrin and NACHT domains are both essential for NLRC3-like function. The requirement for the pyrin domain supports the possibility that NLRC3-like may functionally interact with other pyrin-containing proteins such as ASC (Dorfleutner et al., 2007a; Vajjhala et al., 2012; Liepinsh et al., 2003), and the requirement for the NACHT domain indicates that NLRC3-like may also interact with itself or other NLR proteins that regulate inflammatory signaling.

LPS Challenge Compromises Microglia Development in *nlrc3-like* Heterozygous Embryos

To further test the relationship between systemic immune activation and *nlrc3-like* function, we injected LPS into the bloodstream of embryos from *nlrc3-like*$^{+/-}$ heterozygous intercrosses at 1 and 2 dpf and analyzed microglial development at 3 dpf. LPS injection reduced microglia formation in many of the injected *nlrc3-like*$^{+/-}$ heterozygous embryos (54%, n = 24) and affected one of nine injected wild-type siblings (11%) (Figure 7). These data indicate that *nlrc3-like*$^{+/-}$ heterozygotes are more susceptible to disruptions of microglia development when exposed to the LPS inflammatory stimulus than wild-type siblings. These results are consistent with the autonomous function of *nlrc3-like* in the macrophage lineage (Figures 5A and 5B) but also show that extrinsic inflammatory stimuli can disrupt the development of microglia when *nlrc3-like* function is partially reduced.

DISCUSSION

Macrophages utilize an array of pattern-recognition receptors, including the Toll-like receptors (TLRs) and NLRs, to recognize and respond rapidly to infection, injury, and cellular stress (Chen et al., 2009; Davis et al., 2011; Mosser and Edwards, 2008). The signaling activities of these receptors must be regulated to maintain homeostasis and prevent inappropriate or chronic inflammation. Previous studies show that TLR signaling is attenuated through multiple mechanisms, including production of decoy receptors and inhibitors of downstream signaling complexes (Anwar et al., 2013; Coll and O'Neill, 2010). Much less is known about the negative regulation of NLRs in vivo,

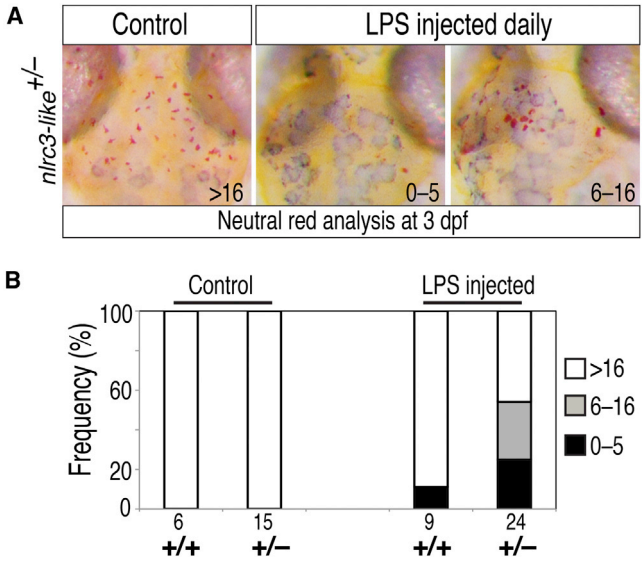

Figure 7. Exposure of *nlrc3-like* Heterozygous Embryos to Systemic LPS Challenge Disrupts Microglia Development

(A) Neutral red staining at 3 dpf shows normal formation of microglia in control uninjected *nlrc3-like* heterozygous embryos. In contrast, many *nlrc3-like* heterozygous embryos injected with LPS at 1 and 2 dpf have strongly reduced (6–16 microglia) or eliminated (0–5 microglia) microglia.

(B) Bar graph shows the frequency of loss of microglia in *nlrc3-like* heterozygous fish injected with LPS, compared with little effect on the wild-type siblings.

despite their critical roles in controlling innate immunity (Chen et al., 2009; Davis et al., 2011; Coll and O'Neill, 2010). Our results demonstrate that *nlrc3-like* is an essential negative regulator of macrophage activation and inflammation. Loss of NLRC3-like causes an inflammatory state in macrophages that profoundly alters their normal course of development. Instead of seeding the brain to form microglia, embryonic macrophages in the mutant actively migrate to form aberrant cellular aggregations in the yolk, fail to enter the brain, and eventually undergo inflammatory cell death. Activity of *nlrc3-like* continues to be required even after microglial progenitors enter the brain and differentiate because transient expression of the wild-type gene is not sufficient for long-term rescue of microglia or suppression of inflammation. These results highlight the importance of regulating the activation of embryonic macrophages to allow normal microglia development, in addition to the more widely recognized need to control activation of adult microglia to prevent chronic or acute inflammation that is common in many neurodegenerative and autoimmune diseases such as Alzheimer's disease, Parkinson's disease, and multiple sclerosis (Cunningham, 2013; Amor et al., 2010).

Our data support a model in which NLRC3-like competes with proinflammatory NLRs for ASC binding to set a threshold level of activated canonical NLRs required to trigger inflammation. According to this view, NLRC3-like would prevent widespread inflammation in response to limited or transient stimuli, such as exposure to nonpathogenic microbes, but still allow rapid initiation of inflammation when NLRs are activated by a robust stimulus such as an injury or infection. This model is also consistent with the proposed mechanism of cellular and viral proteins containing only the pyrin domain, only the NACHT domain, or a pyrin and NACHT, which inhibit the inflammasome through homotypic binding (Dorfleutner et al., 2007a, b; Imamura et al., 2010; Stehlik et al., 2003). Furthermore, similar to these inflammasome inhibitory proteins, NLRC3-like has a distinctive pyrin-NACHT structure that lacks the canonical LRRs thought to be important for self-inhibition (Rosenstiel et al., 2007; Chen et al., 2009), suggesting that it may be a constitutively active inhibitor. Our structure-function analysis indicates that both the pyrin and NACHT domains are required for NLRC3-like function, suggesting that NLRC3-like may interact with other proteins containing one or both of these domains, including the adaptor ASC.

The zebrafish genome contains a large number of NLR genes homologous to mammalian NLRC3 (Laing et al., 2008), and our analysis provides functional insights into this group of zebrafish NLRC3-like genes. Although its NACHT domain is most similar to the mammalian NLRC3 (Laing et al., 2008; Hughes, 2006), the central NACHT domain is the only major region conserved between the zebrafish NLRC3-like and mammalian NLRC3 proteins. Moreover, the zebrafish NLRC3-like protein has only pyrin and NACHT domains, whereas the mammalian NLRC3 has C-terminal LRRs but lacks an N-terminal effector motif. Our biochemical studies suggest that zebrafish NLRC3-like may suppress inflammation by interfering with interactions between ASC and other inflammasome components. The mammalian NLRC3 protein can also suppress inflammation. A recent study shows that NLRC3 reduces TLR signaling and NF-κB activity after LPS exposure through its interaction with TRAF6 (Schneider et al., 2012). It is also possible that zebrafish NLRC3-like regulates NF-κB activation in an inflammasome-independent manner because highly elevated levels of mRNAs for proinflammatory cytokines were detected in *nlrc3-like*-deficient embryos. Consistent with this possibility, zebrafish NLRC3-like has three predicted TRAF-interaction motifs (following the consensus Pro/Ser/Ala/Thr-X-Gln/Glu-Glu). Thus, NLRC3-like may repress NF-κB activity by interference with TRAF adaptor proteins in the recruitment of NF-κB, similar to the anti-inflammatory action of NLRC3 and NLRP12 after immune stimulation (Schneider et al., 2012; Allen et al., 2012; Zaki et al., 2011). Alternatively, inappropriate activation of the inflammasome may secondarily induce cytokine expression in *nlrc3-like* mutants.

Another important and intriguing difference between zebrafish *nlrc3-like* and the mouse NLR genes known to suppress inflammation, including NLRC3 and NLRP12 (Schneider et al., 2012; Allen et al., 2012; Zaki et al., 2011), is that the mouse hyperinflammatory mutant phenotypes are evident only after LPS injection or infection, whereas systemic inflammation is found in *nlrc3-like* mutant zebrafish in the absence of immune perturbation. Under standard rearing conditions, wild-type and heterozygous siblings show no signs of inflammation, but *nlrc3-like* mutants display severe, systemic dysregulation of the immune system. This difference reveals that *nlrc3-like* is an essential suppressor of inflammation at steady state, highlighting the importance of the regulatory mechanism that controls immune activation not only in response to overt immune challenges but also during normal development.

In summary, we identify an essential role for an NLR that acts as a checkpoint on inflammatory processes and permits the development of microglia in zebrafish. Our analysis of *nlrc3-like* mutants highlights the deleterious effect that inflammatory activation has on embryonic macrophages and their subsequent development into microglia. The negative regulatory function of NLRC3-like may provide important insights into the maintenance of homeostasis and the etiology of autoimmune and inflammatory disorders.

EXPERIMENTAL PROCEDURES

Zebrafish Lines and Embryos

Experimental protocols involving zebrafish were approved by the Stanford University Institutional Animal Care and Use Committee. Embryos from wild-type (TL, AB/TU, and WIK), *Tg(lyz:EGFP)* (Hall et al., 2007), *Tg(mpeg1:EGFP)* (Ellett et al., 2011), *Tg(kdrl:mCherry-CAAX)* (Fujita et al., 2011), *Tg(pu.1:Gal4-UAS-EGFP)* (Peri and Nüsslein-Volhard, 2008), and *nlrc3-like*$^{st73/+}$ strains were raised at 28.5°C and staged as described by Kimmel et al. (1995). Embryos were treated with 0.003% 1-phenyl-2-thiourea (PTU) in methylene blue embryo water to inhibit pigmentation.

ENU Mutagenesis, Microglia Screen, and Neutral Red Assay

Founder P0 wild-type males were mutagenized with N-ethyl-N-nitrosourea (ENU) and subsequently outcrossed to raise F1 and F2 families for screening as described by Pogoda et al. (2006). A pilot F3 genetic screen was conducted to identify putative mutants with specific defects in microglia (e.g., loss of microglia), but no apparent anatomical morphological defects at 5 dpf. A total of 74 F2 families were screened, which amounted to analysis of 50.7 mutagenized genomes. Two putative microglia mutants were identified, but only *st73* was recovered. Microglia were scored in the live larvae by a neutral red vital dye-staining assay (Herbomel et al., 2001) with modifications. For phenotypic analyses, neutral red assay was used at 3 dpf and later stages by incubating larvae in embryo water containing 2.5 μg/ml neutral red at 28.5°C for 2–3 hr, followed by one to two water changes, and then analyzed 0.5–24 hr later using a dissecting microscope.

Genetic Mapping

st73 mutant embryos were phenotypically sorted from wild-type siblings at 4–5 dpf by a lack of neutral red-positive microglia staining in the head. Bulk segregant analysis with 480 simple sequence length polymorphisms (SSLPs) (Talbot and Schier, 1999) identified markers on LG15 flanking the *st73* mutation. High-resolution mapping was conducted using additional SSLPs and single-nucleotide polymorphisms linked to the mutation, which were found from sequencing PCR fragments amplified from genomic DNA of mutants and wild-type siblings. Sequencing segments of genes in the critical interval by PCR from genomic DNA templates identified the *st73* lesion in the *nlrc3-like* gene (LOC100538217). Genotyping the *st73* lesion is based on a PCR/restriction digest assay using the following forward and reverse PCR primers and MseI digest: 5′-CAACAATTTCATCAAAATCTTCAA-3′ and 5′-CAGACATATT CTGGAAGCAAACA-3′, respectively.

Whole-Mount RNA In Situ Hybridization

In situ hybridization on whole-zebrafish embryos and larvae from 20 hpf to 5 dpf was performed using standard methods as described by Pogoda et al. (2006). Antisense riboprobes were transcribed from the following gene-coding sequences cloned in pCRII-Topo vector: *lyz* (518 bp); *mfap4* (627 bp using primer sequences as described by Zakrzewska et al., 2010); *l-plastin* (1,541 bp of *lcp1*); and *apoe* (505 bp of *apoeb*). Other probes were made from vectors encoding *mpo* (full-length, Open Biosystems clone 6960294) and *kdrl* (*flk1*) (Thisse et al., 2008).

Whole-Mount Immunostaining and TUNEL Assay

TUNEL assay (In Situ Cell Death Detection Kit, TMR red; Roche) was performed as previously described by Chen et al. (2010). Subsequent immunostaining on whole-zebrafish embryos or larvae was performed using the anti-L-plastin (Redd et al., 2006) at 1:250–500 dilution and anti-GFP (GT859; GeneTex) at 1:500 dilution, followed by DAPI staining.

Time-Lapse and Fluorescent Imaging

For live imaging, embryos were embedded in 1.5% low-melting point agarose on glass slides. For cryosectioning, postfixed embryos were equilibrated to 30% sucrose, embedded in OCT medium, snap frozen in dry ice-ethanol bath, sectioned at 10–12 μm, and subsequently imaged. All time-lapse and fluorescent images, except images for analysis of vacuolation and apoptosis, were taken on a Zeiss LSM 5 Pascal confocal microscope using the 10× (NA 0.30) and 20× (NA 0.75) objectives, and 488 and 543 nm laser lines with bright field. Images of yolk sac macrophages for assessing cellular vacuolation and cell death were taken on an upright Zeiss Axio Imager.M2 microscope using the 20× (NA 0.8) and 63× (NA 1.4) plan-apochromatic objectives. See also the Supplemental Experimental Procedures for additional information.

Expression Constructs

Full-length *nlrc3-like*-coding sequence (XM_003200091.1) was cloned from a 2.5 dpf embryonic cDNA pool and directionally inserted into the pCS2+ plasmid at XhoI/XbaI sites to make pCS2-FL-nlrc3-like for mRNA transcription. Truncated forms (pCS2-nlrc3-like-Δpyrin and pCS2-nlrc3-like-ΔNACHT) were made using fusion PCR and also directionally cloned into the pCS2+ plasmid at XhoI/XbaI sites. All transgenic expression constructs contained the Tol2-transposon sequences for genomic integration. Primers used in cloning are listed in Table S1. See also Supplemental Experimental Procedures for further details.

mRNA, Plasmid, and MO Injections

pCS2-FL-nlrc3-like and truncated forms (pCS2-nlrc3-like-Δpyrin and pCS2-nlrc3-like-ΔNACHT) were transcribed using the Sp6 mMessage machine (Ambion) to produce 5′ capped mRNAs with a poly-A tail. A range of 50–200 pg of *nlrc3-like* mRNA was injected into one- to four-cell stage embryos; all amounts of RNA tested in this range can rescue microglia in *nlrc3-like* mutants. Structure-function analysis was conducted using injections of 150–200 pg of mRNA in one- to two-cell stage embryos. Transgenes were transiently expressed by coinjecting ~12–25 pg of Tol2 plasmid as described above and ~50–100 pg of Tol2 transposase mRNA at one-cell stage. A splice-blocking MO against *irf8* was synthesized by Gene Tools and was injected at 2.5–5 ng into one-cell stage embryos as previously described by Li et al. (2011). As negative controls, embryos were injected with water or not injected.

RNA Extraction, RT-PCR, and qPCR

Total RNA was extracted from individual embryos using the RNAqueous-Micro RNA Isolation Kit (Ambion). Embryos were presorted by neutral red phenotype prior to lysis and genotyped using a PCR-restriction digest assay as described above. cDNA was made using oligo dT primer and SuperScript II or III Reverse Transcriptase (Invitrogen). qPCR was performed on the ABI 7300 Real-Time PCR System or the Bio-Rad CFX384 Real-Time PCR Detection System with SYBR GreenER qPCR reagent (Invitrogen). Additional information is provided in the Supplemental Experimental Procedures.

Protein-Interaction Pull-Down Assay

DNA constructs were made using modified Gateway vectors (Meireles et al., 2009). GST-ASC fusion protein containing the full-length zebrafish ASC sequence (NM_131495.2) was made in pGEX-4T-1 vector. Full-length NLRC3-like protein (XP_003200139.1) was fused to MBP using the vector pMAL-c2X. All proteins were expressed in *Escherichia coli* BL-21 cells (Invitrogen) using IPTG induction. See also the Supplemental Experimental Procedures for more details.

LPS Microinjection

A total of 3–5 nl of LPS from *Pseudomonas aeruginosa* 10 (Sigma-Aldrich) at 5 mg/ml in PBS with rhodamine dextran (10,000 MW at 1:5 dilution) was injected into the circulation valley (duct of Cuvier) as described by Milligan-Myhre et al. (2011). Embryos were injected at 22–24 hpf and at 48 hpf;

detection of the fluorescent dextran throughout vasculature was used to select for successful injections for later analysis. Injected embryos and control uninjected siblings were analyzed at 3 dpf using the neutral red assay for microglia.

SUPPLEMENTAL INFORMATION

Supplemental Information includes Supplemental Experimental Procedures, five figures, one table, and eight movies and can be found with this article online at http://dx.doi.org/10.1016/j.celrep.2013.11.004.

AUTHOR CONTRIBUTIONS

C.E.S. recovered and mapped the *st73* mutation, and conducted all experiments. K.R.M., W.J., and W.S.T. performed the genetic screen. C.E.S. and W.S.T. analyzed the data and wrote the manuscript.

ACKNOWLEDGMENTS

We are grateful to G.J. Lieschke, A.T. Look, F. Marlow, S. Mercurio, H. Ohkura, F. Peri, M. Redd, B. Weinstein, and G. Wright for fish strains and plasmids; A. Meireles for cloning reagents; and M. Barna, M. Fuller, and S. Kim for sharing equipment. Special thanks to M. Krasnow, A. Schier, B. Barres, and Talbot lab members for critical comments on the manuscript and T. Reyes and C. Hill for fish care. C.E.S. was supported by NIH NRSA postdoctoral fellowship 5F32NS067754, and K.R.M. was supported by NMSS fellowship FG 1719-A-1. This work was supported by NIH grant R01 NS065787 to W.S.T.

Received: June 8, 2013
Revised: September 5, 2013
Accepted: November 4, 2013
Published: December 5, 2013

REFERENCES

Aguzzi, A., Barres, B.A., and Bennett, M.L. (2013). Microglia: scapegoat, saboteur, or something else? Science *339*, 156–161.

Allen, I.C., Wilson, J.E., Schneider, M., Lich, J.D., Roberts, R.A., Arthur, J.C., Woodford, R.M., Davis, B.K., Uronis, J.M., Herfarth, H.H., et al. (2012). NLRP12 suppresses colon inflammation and tumorigenesis through the negative regulation of noncanonical NF-κB signaling. Immunity *36*, 742–754.

Amor, S., Puentes, F., Baker, D., and van der Valk, P. (2010). Inflammation in neurodegenerative diseases. Immunology *129*, 154–169.

Anwar, M.A., Basith, S., and Choi, S. (2013). Negative regulatory approaches to the attenuation of Toll-like receptor signaling. Exp. Mol. Med. *45*, e11.

Chen, G., Shaw, M.H., Kim, Y.G., and Nuñez, G. (2009). NOD-like receptors: role in innate immunity and inflammatory disease. Annu. Rev. Pathol. *4*, 365–398.

Chen, H.L., Yuh, C.H., and Wu, K.K. (2010). Nestin is essential for zebrafish brain and eye development through control of progenitor cell apoptosis. PLoS ONE *5*, e9318.

Coll, R.C., and O'Neill, L.A. (2010). New insights into the regulation of signalling by toll-like receptors and nod-like receptors. J. Innate Immun. *2*, 406–421.

Cunningham, C. (2013). Microglia and neurodegeneration: the role of systemic inflammation. Glia *61*, 71–90.

Davis, B.K., Wen, H., and Ting, J.P. (2011). The inflammasome NLRs in immunity, inflammation, and associated diseases. Annu. Rev. Immunol. *29*, 707–735.

Dorfleutner, A., Bryan, N.B., Talbott, S.J., Funya, K.N., Rellick, S.L., Reed, J.C., Shi, X., Rojanasakul, Y., Flynn, D.C., and Stehlik, C. (2007a). Cellular pyrin domain-only protein 2 is a candidate regulator of inflammasome activation. Infect. Immun. *75*, 1484–1492.

Dorfleutner, A., Talbott, S.J., Bryan, N.B., Funya, K.N., Rellick, S.L., Reed, J.C., Shi, X., Rojanasakul, Y., Flynn, D.C., and Stehlik, C. (2007b). A Shope Fibroma virus PYRIN-only protein modulates the host immune response. Virus Genes *35*, 685–694.

Ellett, F., Pase, L., Hayman, J.W., Andrianopoulos, A., and Lieschke, G.J. (2011). mpeg1 promoter transgenes direct macrophage-lineage expression in zebrafish. Blood *117*, e49–e56.

Fujita, M., Cha, Y.R., Pham, V.N., Sakurai, A., Roman, B.L., Gutkind, J.S., and Weinstein, B.M. (2011). Assembly and patterning of the vascular network of the vertebrate hindbrain. Development *138*, 1705–1715.

Ginhoux, F., Greter, M., Leboeuf, M., Nandi, S., See, P., Gokhan, S., Mehler, M.F., Conway, S.J., Ng, L.G., Stanley, E.R., et al. (2010). Fate mapping analysis reveals that adult microglia derive from primitive macrophages. Science *330*, 841–845.

Hall, C., Flores, M.V., Storm, T., Crosier, K., and Crosier, P. (2007). The zebrafish lysozyme C promoter drives myeloid-specific expression in transgenic fish. BMC Dev. Biol. *7*, 42.

Herbomel, P., Thisse, B., and Thisse, C. (1999). Ontogeny and behaviour of early macrophages in the zebrafish embryo. Development *126*, 3735–3745.

Herbomel, P., Thisse, B., and Thisse, C. (2001). Zebrafish early macrophages colonize cephalic mesenchyme and developing brain, retina, and epidermis through a M-CSF receptor-dependent invasive process. Dev. Biol. *238*, 274–288.

Hughes, A.L. (2006). Evolutionary relationships of vertebrate NACHT domain-containing proteins. Immunogenetics *58*, 785–791.

Imamura, R., Wang, Y., Kinoshita, T., Suzuki, M., Noda, T., Sagara, J., Taniguchi, S., Okamoto, H., and Suda, T. (2010). Anti-inflammatory activity of PYNOD and its mechanism in humans and mice. J. Immunol. *184*, 5874–5884.

Kimmel, C.B., Ballard, W.W., Kimmel, S.R., Ullmann, B., and Schilling, T.F. (1995). Stages of embryonic development of the zebrafish. Dev. Dyn. *203*, 253–310.

Kolly, L., Karababa, M., Joosten, L.A., Narayan, S., Salvi, R., Pétrilli, V., Tschopp, J., van den Berg, W.B., So, A.K., and Busso, N. (2009). Inflammatory role of ASC in antigen-induced arthritis is independent of caspase-1, NALP-3, and IPAF. J. Immunol. *183*, 4003–4012.

Lage, S.L., Amarante-Mendes, G.P., and Bortoluci, K.R. (2013). Evaluation of pyroptosis in macrophages using cytosolic delivery of purified flagellin. Methods *61*, 110–116.

Laing, K.J., Purcell, M.K., Winton, J.R., and Hansen, J.D. (2008). A genomic view of the NOD-like receptor family in teleost fish: identification of a novel NLR subfamily in zebrafish. BMC Evol. Biol. *8*, 42.

Lam, S.H., Chua, H.L., Gong, Z., Lam, T.J., and Sin, Y.M. (2004). Development and maturation of the immune system in zebrafish, *Danio rerio*: a gene expression profiling, in situ hybridization and immunological study. Dev. Comp. Immunol. *28*, 9–28.

Lamkanfi, M., and Dixit, V.M. (2010). Manipulation of host cell death pathways during microbial infections. Cell Host Microbe *8*, 44–54.

Li, L., Jin, H., Xu, J., Shi, Y., and Wen, Z. (2011). Irf8 regulates macrophage versus neutrophil fate during zebrafish primitive myelopoiesis. Blood *117*, 1359–1369.

Liepinsh, E., Barbals, R., Dahl, E., Sharipo, A., Staub, E., and Otting, G. (2003). The death-domain fold of the ASC PYRIN domain, presenting a basis for PYRIN/PYRIN recognition. J. Mol. Biol. *332*, 1155–1163.

Mason, D.R., Beck, P.L., and Muruve, D.A. (2012). Nucleotide-binding oligomerization domain-like receptors and inflammasomes in the pathogenesis of non-microbial inflammation and diseases. J. Innate Immun. *4*, 16–30.

Meijer, A.H., and Spaink, H.P. (2011). Host-pathogen interactions made transparent with the zebrafish model. Curr. Drug Targets *12*, 1000–1017.

Meireles, A.M., Fisher, K.H., Colombié, N., Wakefield, J.G., and Ohkura, H. (2009). Wac: a new Augmin subunit required for chromosome alignment but not for acentrosomal microtubule assembly in female meiosis. J. Cell Biol. *184*, 777–784.

Milligan-Myhre, K., Charette, J.R., Phennicie, R.T., Stephens, W.Z., Rawls, J.F., Guillemin, K., and Kim, C.H. (2011). Study of host-microbe interactions in zebrafish. Methods Cell Biol. *105*, 87–116.

Moore, K.W., de Waal Malefyt, R., Coffman, R.L., and O'Garra, A. (2001). Interleukin-10 and the interleukin-10 receptor. Annu. Rev. Immunol. *19*, 683–765.

Mosser, D.M., and Edwards, J.P. (2008). Exploring the full spectrum of macrophage activation. Nat. Rev. Immunol. *8*, 958–969.

Mujawar, Z., Rose, H., Morrow, M.P., Pushkarsky, T., Dubrovsky, L., Mukhamedova, N., Fu, Y., Dart, A., Orenstein, J.M., Bobryshev, Y.V., et al. (2006). Human immunodeficiency virus impairs reverse cholesterol transport from macrophages. PLoS Biol. *4*, e365.

Paolicelli, R.C., Bolasco, G., Pagani, F., Maggi, L., Scianni, M., Panzanelli, P., Giustetto, M., Ferreira, T.A., Guiducci, E., Dumas, L., et al. (2011). Synaptic pruning by microglia is necessary for normal brain development. Science *333*, 1456–1458.

Peri, F., and Nüsslein-Volhard, C. (2008). Live imaging of neuronal degradation by microglia reveals a role for v0-ATPase a1 in phagosomal fusion in vivo. Cell *133*, 916–927.

Perry, V.H., Nicoll, J.A., and Holmes, C. (2010). Microglia in neurodegenerative disease. Nat Rev Neurol *6*, 193–201.

Pogoda, H.M., Sternheim, N., Lyons, D.A., Diamond, B., Hawkins, T.A., Woods, I.G., Bhatt, D.H., Franzini-Armstrong, C., Dominguez, C., Arana, N., et al. (2006). A genetic screen identifies genes essential for development of myelinated axons in zebrafish. Dev. Biol. *298*, 118–131.

Ransohoff, R.M., and Cardona, A.E. (2010). The myeloid cells of the central nervous system parenchyma. Nature *468*, 253–262.

Ransohoff, R.M., and Perry, V.H. (2009). Microglial physiology: unique stimuli, specialized responses. Annu. Rev. Immunol. *27*, 119–145.

Redd, M.J., Kelly, G., Dunn, G., Way, M., and Martin, P. (2006). Imaging macrophage chemotaxis in vivo: studies of microtubule function in zebrafish wound inflammation. Cell Motil. Cytoskeleton *63*, 415–422.

Renshaw, S.A., and Trede, N.S. (2012). A model 450 million years in the making: zebrafish and vertebrate immunity. Dis. Model. Mech. *5*, 38–47.

Rock, K.L., Latz, E., Ontiveros, F., and Kono, H. (2010). The sterile inflammatory response. Annu. Rev. Immunol. *28*, 321–342.

Rosenstiel, P., Till, A., and Schreiber, S. (2007). NOD-like receptors and human diseases. Microbes Infect. *9*, 648–657.

Sarkar, A., Duncan, M., Hart, J., Hertlein, E., Guttridge, D.C., and Wewers, M.D. (2006). ASC directs NF-kappaB activation by regulating receptor interacting protein-2 (RIP2) caspase-1 interactions. J. Immunol. *176*, 4979–4986.

Schafer, D.P., Lehrman, E.K., Kautzman, A.G., Koyama, R., Mardinly, A.R., Yamasaki, R., Ransohoff, R.M., Greenberg, M.E., Barres, B.A., and Stevens, B. (2012). Microglia sculpt postnatal neural circuits in an activity and complement-dependent manner. Neuron *74*, 691–705.

Schneider, M., Zimmermann, A.G., Roberts, R.A., Zhang, L., Swanson, K.V., Wen, H., Davis, B.K., Allen, I.C., Holl, E.K., Ye, Z., et al. (2012). The innate immune sensor NLRC3 attenuates Toll-like receptor signaling via modification of the signaling adaptor TRAF6 and transcription factor NF-κB. Nat. Immunol. *13*, 823–831.

Siracusa, M.C., Reece, J.J., Urban, J.F., Jr., and Scott, A.L. (2008). Dynamics of lung macrophage activation in response to helminth infection. J. Leukoc. Biol. *84*, 1422–1433.

Stehlik, C., Krajewska, M., Welsh, K., Krajewski, S., Godzik, A., and Reed, J.C. (2003). The PAAD/PYRIN-only protein POP1/ASC2 is a modulator of ASC-mediated nuclear-factor-kappa B and pro-caspase-1 regulation. Biochem. J. *373*, 101–113.

Talbot, W.S., and Schier, A.F. (1999). Positional cloning of mutated zebrafish genes. Methods Cell Biol. *60*, 259–286.

Thisse, B., Wright, G.J., and Thisse, C. (2008). Embryonic and larval expression patterns from a large scale screening for novel low affinity extracellular protein interactions. ZFIN Direct Data Submission. http://zfin.org.

Vajjhala, P.R., Mirams, R.E., and Hill, J.M. (2012). Multiple binding sites on the pyrin domain of ASC protein allow self-association and interaction with NLRP3 protein. J. Biol. Chem. *287*, 41732–41743.

Zaki, M.H., Vogel, P., Malireddi, R.K., Body-Malapel, M., Anand, P.K., Bertin, J., Green, D.R., Lamkanfi, M., and Kanneganti, T.D. (2011). The NOD-like receptor NLRP12 attenuates colon inflammation and tumorigenesis. Cancer Cell *20*, 649–660.

Zakrzewska, A., Cui, C., Stockhammer, O.W., Benard, E.L., Spaink, H.P., and Meijer, A.H. (2010). Macrophage-specific gene functions in Spi1-directed innate immunity. Blood *116*, e1–e11.